Imaging of Coherent Source Distribution in the Near Field

Ryo Nishimoto, Yoshihiko Kuwahara

Graduate School of Engineering, Shizuoka University

3-5-1 Johoku Nakaku Hamamatsu 432-8561 Japan, tykuwab@ipc.shizuoka.ac.jp

Abstract

We propose a method to image the distribution of coherent sources in the near field by the inverse problem with Tihknov regularization. Elements for Jacobian are calculated by the adjoint method. Node which has a weak wave source is iteratively removed in order to enhance the contrast.

Keywords : Inverse Problem Adjoint Method Tihknov Regularization Contrast Enhancement

1. Introduction

For the electromagnetic interference problems, a technology which can identify plural coherent sources in the near field is required. The super-resolution technology can estimate the direction of the arrival in the near field with high resolution. However, it is difficult to resolve coherent sources in the near field [1]. Also, it is difficult to estimate a steering vector in the strange area.

In this article, in order to image the distribution of coherent sources in the near field a method by the inverse problem with Tihknov regularization is proposed. This type of technology has been studied in the field of active imaging such as the microwave tomography [2]. We modify it for passive imaging. In the proposed method, a regularization coefficient is found from the inflection point of L-curve [3], Elements of Jacobian are calculated by the adjoint method and the contrast of the reconstructed image is enhanced by removing weak source area iteratively. It is demonstrated by numerical simulation that plural coherent sources in the near field can be identified.

2. 2D FEM

We analyze 2D electromagnetic field including several point sources by the finite-element method (FEM). It is supposed that the electric field E only exists along z-axis. We denote wave number in the free-space, angular frequency, permeability in the free-space, and source as k_0, ω, μ_0, and J_z. The analysis space is divided by Ne triangular elements. When a basis function for an triangular element ϕ_l is applied to each element, the weak-form of Helmholtz equation is expressed by [4] ,

$$\langle \nabla E_z, \nabla \phi_l \rangle - \langle k_0^2 \nabla E_z, \nabla \phi_l \rangle - \oint_\Gamma \frac{\partial E_z}{\partial n} \phi_l d\Gamma = \langle - j\omega\mu_0 J_z, \phi_l \rangle \quad (1)$$

Where, $\langle , \rangle$, n, and Γ denote surface integral for each element, normal vector, edge of the surface, respectively. When E_z is expanded by a basis function and contribution of all elements in the analysis space is summed, the problem results in a linear simultaneous equation.

$$[\mathbf{A}]\{\mathbf{E}_z\} = \{\mathbf{b}_z\} \quad (2)$$

where,

$$a_{il} = \langle \nabla \phi_i, \nabla \phi_l \rangle - \langle k^2 \phi_i, \phi_l \rangle \quad (2a)$$

$$b_z^l = \langle - j\omega\mu_0 J_z, \phi_l \rangle \quad (2b)$$

By solving (2), the complex electric field E_z of each node can be achieved. Also, the absorption boundary condition (ABC) must be set. In this paper, Bayliss Gunzburger Turkel (BGT) [4] was used.

3. Inverse Problem

3.1 Tikhonov Regulization

We reconstruct an image by Tikhonov regularization. The functional is defined as

$$f(\mathbf{J}_z) = \left\| \mathbf{E}_z^{meas} - \mathbf{E}_z^{calc}(\mathbf{J}_z) \right\|_2^2 + \lambda^2 \left\| \mathbf{J}_z \right\|_2^2 \tag{3}$$

Where, $\mathbf{E}_z^{meas}$, $\mathbf{E}_z^{calc}(\mathbf{J}_z)$, and λ denote measured electric field, estimated electric field in process of the image reconstruction, and regularization factor. Source J_z is assigned to each node.

$$J_z(x, y) = J_z \cdot \delta(x, y) \tag{4}$$

We estimate a group of J_z which minimizes (3). Variation $\delta \mathbf{J}_z$ to approach a set value to the true value is expressed by,

$$\delta \mathbf{J}_z = \arg \min_{\delta J_z} \left\{ \left\| \mathbf{J}_M(\mathbf{J}_z)\delta \mathbf{J}_z - \left(\mathbf{E}^{meas} - \mathbf{E}^{calc}(\mathbf{J}_z) \right) \right\|_2^2 + \lambda^2 \left\| \mathbf{J}_z \right\|_2^2 \right\} \tag{5}$$

Where, $\mathbf{J}_M$ is Jacobian of $\mathbf{E}^{calc}(J_z)$. $\mathbf{J}_z$ can be estimated by next recursive formulas [5],

$$\mathbf{J}_z^{k+1} = \mathbf{J}_z^k + \delta \mathbf{J}_z \tag{6}$$

$$\delta \mathbf{J}_z = \left(\mathbf{J}_M^H \mathbf{J}_M + \lambda^2 \mathbf{I} \right)^{-1} \mathbf{J}_M^H \left\{ \mathbf{E}^{meas} - \mathbf{E}^{calc}(\mathbf{J}_z) \right\}$$

Here, we initialize as $\mathbf{J}_z^1 = \mathbf{0}$, that is, we have not any information beforehand.

3.2 Calculation of Jacobian by the adjoint method

When a source exists in, an element of Jacobian in which the electric field on $r = (x_r, y_r)$ is differentiated by a source on node n is expressed by,

$$J_M(\mathbf{r}, n) = \left\langle \frac{\partial E_z^r}{\partial J_z^n}, \delta(x_r, y_r) \right\rangle \tag{7}$$

On the other hand, when we differentiate both sides of (2) by J_z^n,

$$[\mathbf{A}] \left\{ \frac{\partial \mathbf{E}_z}{\partial J_z^n} \right\} = \left\{ \frac{\partial \mathbf{b}_z}{\partial J_z^n} \right\} \tag{8}$$

When a source exists in r,

$$[\mathbf{A}] \left\{ \mathbf{E}_z^r \right\} = \left\{ \mathbf{b}_r \right\} \tag{9}$$

From (8),(9) following relation can be achieved.

$$\left\langle [\mathbf{A}] \left\{ \frac{\partial \mathbf{E}_z}{\partial J_z^n} \right\}, \mathbf{b}_r \right\rangle = \left\langle [\mathbf{A}] \left\{ \mathbf{E}_z^r \right\}, \left\{ \frac{\partial \mathbf{b}_z}{\partial J_z^n} \right\} \right\rangle \tag{10}$$

For each element of (10), we integrate it over the related element surface. Using 2(b), we modify (10). Then, an element of (10) is expressed by,

$$\left\langle \frac{\partial E_z^l}{\partial J_z^n}, \left\langle - j\omega\mu_0 J_z^r \delta(x_r, y_r), \phi_l \right\rangle \right\rangle = \left\langle E_z^r, \left\langle - j\omega\mu_0, \phi_l \right\rangle \right\rangle \tag{11}$$

We integrate an element over the related surface.

$$\left\langle \frac{\partial E_z}{\partial J_z^n}, \frac{S^{(e)}}{3} J_z^r \delta(x_r, y_r) \right\rangle = \left\langle E_z^r, \frac{S^{(e')}}{3} \right\rangle \tag{12}$$

Where, $S^{(e)}$ is an element area of which node in position of (x, y) is shared by the related element and $S^{(e')}$ is an element area of which node for source is shared. When the area of each element is the same and electric field distribution in the condition of $J_z^r = 1$ is denoted as $E_z^r \big|_{J_z^r = 1}$, an element of Jacobian is expressed by,

$$\left\langle \frac{\partial E_z^r}{\partial J_z^n}, \delta(x_r, y_r) \right\rangle = E_z^r \big|_{J_z^r = 1} \tag{13}$$

3.3　Decision of the regularization coefficient by L-curve

In the inverse problem, the noise and measurement error have serious influence on the result. To reduce such errors, a regularization parameter is decided by L-curve [3]. The approximate solution norm $\left\|\mathbf{J}_z\right\|_2^2$ and residual norm $\left\|\mathbf{E}^{meas} - \mathbf{E}^{calc}(\mathbf{J}_z)\right\|_2^2$ are assigned to the vertical and horizontal axis, respectively. L curve is drawn by varying regularization parameter λ. It is known that L-curve has a corner and that λ which makes curvature the highest is an appropriate regularization parameter.

3.4　Enhancement of the contrast

Generally, contrast of the reconstructed image increases as the analysis space is narrow [7]. In addition, real source should exist in the position where a group of strong wave sources exist while it should exist where a group of weak sources exist. Considering above things, we enhance contrast by the following procedure.
(1) Reconstruct image over the set analysis space.
(2) Specify positions of the source with small energy in the reconstructed image.
(3) Remove nodes with small energy of (2). Then, reconstruct image by the remained node.
(4) Repeat (2) and (3)
As for (2), 10 % of nodes of the lower rank are removed. The residual norm increases compared with that before iteration, it is considered that operation of the removal is not right. In this case, the operation is discarded.

4. Simulation

We have carried out numerical experiments to confirm the effectiveness of the proposed scheme. Simulation conditions are shown in Table 1.

Table1: Simulation Conditions

Frequency	300MHz
Number of receiving antennas	64
Position of receiving antennas	Equi-space on circle of radius of $0.8\,\lambda$
Number of nodes	4185
Search area	radius of $0.7\,\lambda$
Analysis area	radius of λ
Noise level	2% (to the measured signal)
Initial condition	$J_z = 0$
Number of meshes	10201
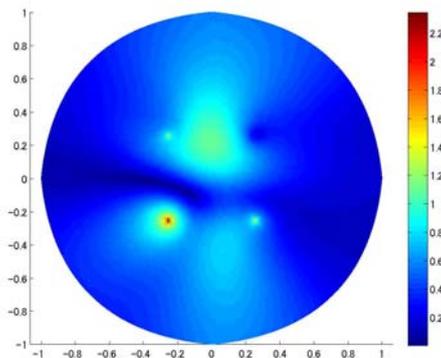
Position of Jz		J(x,y)
X[m]	Y[m]	値
0.25	0.25	1-j
0.25	-0.25	2+j
-0.25	0.25	1-2j
-0.25	-0.25	1+3j

Figure 1: Simulation Model

4 point sources with different complex-amplitude are located on vertex of a square with side of 0.5m. Fig. 1 shows absolute value distribution of the electric field generated by these sources. Reconstructed image on sources is shown in Fig.2. We can see that positions and complex amplitude can be estimated accurately.
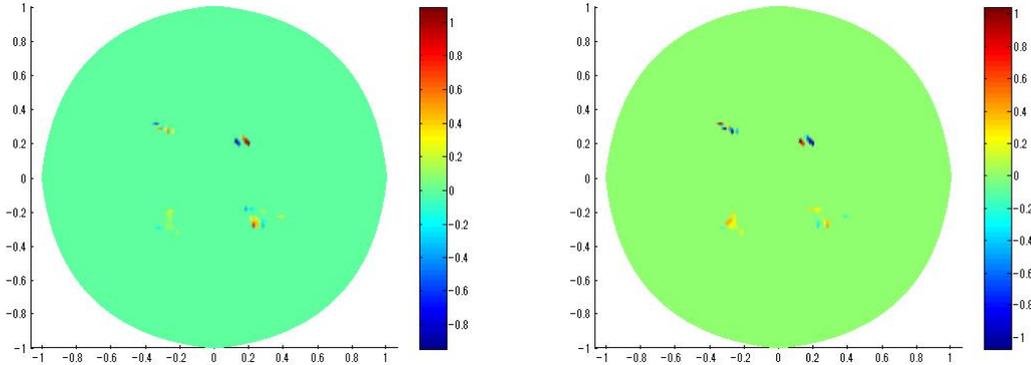
Position of Jz		J(x,y)	
X[m]	Y[m]	Set values	Reconstructed Value
0.25	0.25	1-j	1.005 - 0.977i
0.25	-0.25	2+j	1.998 + 1.016i
-0.25	0.25	1-2j	0.997 - 1.975i
-0.25	-0.25	1+3j	1.001 + 3.011i

Fig.2 Reconstructed Image

5. Conclusions

We propose a method to image distribution of coherent sources in the near field by the inverse problem with Tihknov regularization. Elements for Jacobian are calculated by the adjoint method. Node which has a weak wave source is iteratively removed in order to enhance the contrast. It has been demonstrated by numerical simulation that plural coherent sources in the near field can be identified accurately.

References

[1] S. Yagitani , et al, Localization of Low Frequency Electromagnetic Source, IEICE Trans. Vol.J87-B No.8 pp.1085-93, 2004.
[2] T. Rubaek, et al, Nonlinear microwave imaging for breast cancer screening using Gauss-Newtons method and CGLS inversion algorithm, IEEE Tran. Antennas Propagat. vol.55, no.8, pp.2320-31, 2007.
[3] D.Calvetti, P.C.Hansen and L.Reichel, L-curve curvature bounds via lanczos bidiagonalization, ETNA, vol.14, pp.20-35, 2002.
[4] Giuseppe Pelosi, Roberto Coccioli and Stefano Selleri, *QUICK FINITE ELEMENTS FOR ELECTROMAGNETC WAVE* 2nd ed. Artech House, 2009.
[5] David S Holder, *ELECTRICAL IMPEDANCE TOMOGRAPHY*, IOP Publishing, 2005.
[6] Meaney PM, Paulsen KD, Pogue BW and Miga MI, Microwave image reconstruction utilizing log-magnitude and unwrapped phase to improve high contrast object recovery, *IEEE Trans. Med.Imag.*, vol. 20, pp.104-116, 2001.
[7] Dun Li, Paul M.Meaney, Keith D.Paulsen, Conformal Microave Imaging for Breast Cancer Detection, IEEE Trans. Microwave Theory Tech, vol.51, pp.1179-1186, 2003.